The Journal of Immunology

NF-κB and Activator Protein 1 Response Elements and the Role of Histone Modifications in IL-1β-Induced TGF-β1 Gene Transcription

Kang-Yun Lee, Kazuhiro Ito, Ryuji Hayashi, Elen P. I. Jazrawi, Peter J. Barnes and Ian M. Adcock

J Immunol 2006; 176:603-615; ;
doi: 10.4049/jimmunol.176.1.603
http://www.jimmunol.org/content/176/1/603

The Journal of Immunology is published twice each month by
The American Association of Immunologists, Inc.,
1451 Rockville Pike, Suite 650, Rockville, MD 20852

Print ISSN: 0022-1767 Online ISSN: 1550-6606.

NF-κB and Activator Protein 1 Response Elements and the Role of Histone Modifications in IL-1β-Induced TGF-β1 Gene Transcription[1]

Kang-Yun Lee, Kazuhiro Ito, Ryuji Hayashi, Elen P. I. Jazrawi, Peter J. Barnes, and Ian M. Adcock[2]

Abnormal expression of TGF-β1 is believed to play an important role in the pathogenesis of a number of chronic inflammatory and immune lung diseases, including asthma, chronic obstructive pulmonary disease, and pulmonary fibrosis. Gene activation in eukaryotes requires coordinated use of specific cell signals, chromatin modifications, and chromatin remodeling. We studied the roles of the ubiquitous inflammatory transcription factors, NF-κB and AP-1, in activation of the TGF-β1 gene and histone acetylation at the TGF-β1 promoter. IL-1β-induced TGF-β1 protein secretion and mRNA expression were prevented by actinomycin D and were attenuated by the inhibitor of κB kinase 2 inhibitor AS602868 and the JNK inhibitor SP600125, suggesting a degree of transcriptional regulation mediated by the NF-κB and AP-1 pathways. We demonstrated that IL-1β activated the p65 subunit of NF-κB and the c-Jun subunit of AP-1. Using chromatin immunoprecipitation assays, we observed a sequential recruitment of p65 and c-Jun, accompanying ordered elevation of the levels of histone H4 and H3 acetylation and recruitment of RNA polymerase II at distinct regions in the native TGF-β1 promoter. The specific NF-κB and AP-1 binding sites in the TGF-β1 promoter were confirmed by an ELISA-based binding assay, and evidence for histone hyperacetylation in TGF-β1 induction was supported by the observation that the histone deacetylase inhibitor trichostatin A enhanced basal and IL-1β-induced TGF-β1 mRNA expression. Our results suggest that IL-1β-stimulated transcription of TGF-β1 is temporally regulated by NF-κB and AP-1 and involves histone hyperacetylation at distinct promoter sites. *The Journal of Immunology,* **2006, 176: 603–615.**

Transforming growth factor β, composed of three isoforms, TGF-β1, -β2, and -β3, is a multifunctional cytokine that participates in numerous biological processes, including cell proliferation, differentiation, immune modulation, and extracellular matrix production (1, 2). In addition to physiological effects, abnormal expression of TGF-β has been shown to be important in the pathogenesis of several immunoregulated diseases (3). TGF-β1 is the isoform commonly implicated in inflammation and is up-regulated in response to tissue injury (3). Elevated expression of TGF-β1 occurs in a number of inflammatory pulmonary diseases, e.g., chronic obstructive pulmonary disease (4, 5), asthma (6–8), and idiopathic pulmonary fibrosis (9, 10). It is known that the expression of the TGF-β1 gene can be regulated both transcriptionally and post-transcriptionally (11), and that TGF-β1 expression can be induced by proinflammatory cytokines, such as IL-1β, and TNF-α (12–14). However, the molecular mechanisms underlying the regulation of these processes are not fully understood.

Analysis of the 5′ end of the human TGF-β1 gene revealed that the promoter region is very G+C rich, containing neither a TATA box nor a CAAT box, with two major transcription start sites 271 nt from one another and two promoter activities (15). Using reporter gene assays, the transcription factors AP-1 (16) and SV40 early promoter 1 (17) have previously been implicated in the transcriptional induction of TGF-β1. In monocytes from patients with idiopathic myelofibrosis (18) and in fibrosarcoma cells (19), NF-κB RelA antisense oligonucleotides suppress TGF-β1 mRNA expression. However, precise information about the transcriptional regulation of TGF-β remains unclear.

Eukaryotic genes are organized into assemblies of core histone-containing nucleosomes. To regulate gene expression, transcription factors and RNA polymerases must be able to search packed chromatin efficiently, then locate and interact with their target DNA binding sites. Hyperacetylation of histone H3 and H4 was suggested to be associated with active chromatin (20). It has long been known that acetylation of histones by histone acetyltransferases (HATs)[3] is associated with increased gene transcription, whereas hypoacetylation induced by histone deacetylases (HDACs) is associated with suppression of gene expression (21, 22). Recently, transcriptional coactivators such as CREB-binding protein and p300/CREB-binding protein-associated factor, which is activated by the binding of transcription factors, including AP-1 and NF-κB, were shown to have intrinsic HAT activity (23, 24). It was also demonstrated that induction of a gene is a coordinated event, involving an ordered recruitment of DNA-binding factors, remodeling enzymes, and multiple histone-modifying enzymes (25).

Airways Disease Section, National Heart and Lung Institute, Imperial College London, London, United Kingdom

Received for publication March 8, 2005. Accepted for publication October 24, 2005.

The costs of publication of this article were defrayed in part by the payment of page charges. This article must therefore be hereby marked *advertisement* in accordance with 18 U.S.C. Section 1734 solely to indicate this fact.

[1] This work was supported by the Wellcome Trust and an unrestricted grant from GlaxoSmithKline (U.K.).

[2] Address correspondence and reprint requests to Dr. Ian M. Adcock, Airways Disease Section, National Heart and Lung Institute, Imperial College London, Dovehouse Street, London SW3 6LY, U.K. E-mail address: ian.adcock@imperial.ac.uk

[3] Abbreviations used in this paper: HAT, histone acetyltransferase; CDS, coding sequences; ChIP, chromatin immunoprecipitation; HDAC, histone deacetylase; IKK, inhibitor of κB kinase; m, mutant; Pol II, polymerase II; QPCR, quantitative PCR; TSA, trichostatin A; w, wild type.

0022-1767/05/$02.00

In the present study we investigated the nature of transcription factor pathways and histone acetylation connecting the proinflammatory cytokine IL-1β stimulation to TGF-β1 gene activation. We found that IL-1β triggers TGF-β1 gene expression by activating NF-κB and AP-1 pathways. Using chromatin immunoprecipitation (ChIP) assays, we then demonstrated that p65 and c-Jun are recruited to specific regions of the native promoter of the human TGF-β1 gene. Furthermore, we provide evidence that this transcriptional activation correlates to hyperacetylation of histones H3 and H4 on the TGF-β1 promoter.

Materials and Methods

Cell culture

A549 cells were grown to 90% confluence in DMEM containing 10% FCS before incubation for 48 h in serum-free medium to allow synchronization of cell cycling to G_1. Cells were stimulated by IL-1β (0.001–50 ng/ml; R&D Systems Europe) at various times (0–72 h), and the effects of actinomycin D (Calbiochem), the inhibitor of κB kinase 2 (IKK2) inhibitor AS602868 (Serono), the JNK inhibitor SP600125 (Celgene), and the HDAC inhibitor trichostatin A (TSA; Sigma-Aldrich) on baseline and IL-1β-stimulated expression and release of TGF-β1 were measured.

TGF-β1 ELISA

Determination of TGF-β1 release was measured by ELISA (R&D Systems Europe) according to the manufacturer's instructions. For the assay of total TGF-β1, samples to be tested were first activated by 1 N HCl for 10 min, then neutralized by 1.2 N NaOH/0.5 M HEPES at room temperature. In addition, samples were directly assayed for active TGF-β1 without acid activation.

Western blotting

Total cellular proteins were extracted from A549 cells by freeze-thawing samples in Reporter lysis buffer (Promega). One hundred micrograms of total soluble protein extracts were size-fractionated on 12% PAGE gels and transblotted onto nitrocellulose-ECL membranes (Amersham Biosciences). Proteins were detected with rabbit anti-human TGF-β1 (1/200), anti-p65 (1/500; Santa Cruz Biotechnology), or anti-phospho-c-Jun (1/1000; New England Biolabs). After washing, bound Abs were detected using 1/2000 goat anti-rabbit Ab linked to peroxidase, and bound complexes were detected by ECL (Amersham Biosciences) and expressed in relative optical units.

Real-time quantitative RT-PCR (RT-QPCR) and real-time PCR

Total RNA was isolated using the RNeasy Mini Kit (Qiagen). RNA (1.0 μg) was reverse transcribed using random primers with avian myeloblastosis virus reverse transcriptase (Promega) and using conditions provided by the manufacturer. One microliter of each cDNA sample, corresponding to 7.5 ng of total RNA, was used for real-time PCR.

Real-time PCR was performed in a Rotor-Gene 3000TM Four-Channel Multiplexing System (Corbett Research) using the QuantiTect SYBR Green PCR Kit (Qiagen) to quantify TGF-β1, GAPDH mRNA, and immunoprecipitated DNA from ChIP assays. Cycle parameters were 95°C for 15 min to activate HotStar *Taq* DNA polymerase (Qiagen), followed by annealing and extension at 40 cycles of 94°C for 15 s, 60°C for 25 s, and 72°C for 25 s. In the case of TGF-β1 and GAPDH mRNA, an annealing temperature of 56°C was used. TGF-β1 and GAPDH mRNA and immunoprecipitated DNA were quantified by the standard curve method of relative quantification according to instructions provided by Corbett Research. The amount of TGF-β1 mRNA was normalized to GAPDH mRNA, and the amount of DNA in each ChIP sample was normalized to the input. All real-time PCR data were presented as the fold induction from control samples. No RT controls confirmed that PCR products were RNA derived, and gel electrophoresis and melt curve analysis confirmed specificity. The sequences for all primers used in real-time RT-PCR are as follows: TGF-β1 forward, 5′-CCC AGC ATC TGC AAA GCT C-3′; TGF-β1 reverse, 5′-GTC AAT GTA CAG CTG CCG CA-3′; TP1 forward, 5′-GGA GCG GAG GAA GGA GTC-3′; TP1 reverse, 5′-CTC TTC TCC CGA CCA GCT C-3′, TP2 forward, 5′-CTC GCC CTG TAC AAC AGC AC-3′; TP2 reverse, 5′-GGG TTT CCA CCA TTA GCA C-3′; GAPDH forward, 5′-TTC CAG GAG CGA GAT CCC T-3′; and GAPDH reverse, 5′-CAC CCA TGA CGA ACA TGG G-3′. The sequences for all primers used in real-time PCR for ChIP analysis are: κB1 forward, 5′-GCT GCT GTG TGG GGA TAG AT-3′; κB1 reverse, 5′-GGC CCA GTC TTT TCC TCT CT-3′; κB2 forward, 5′-AAC CCA GAG AGG AAA AGA CT-3′; κB2 reverse, 5′-TGC AGG AAA GGA GAG AGA G-3′, κB3 forward, 5′-GCC ATC TCC CTC CCA CCT-3′; κB3 reverse, 5′-CCT CGG CGA CTC CTT CCT-3′; AP-1-1, the same as κB2; AP-1-2 forward, 5′-CAT CTA CAG TGG GGC CGA-3′; AP-1-2 reverse, 5′-ATG CCT TAG CTG GGG TCA-3′; AP-1-3 forward, 5′-TTG TTT CCC AGC CTG ACT CT-3′; AP-1-3 reverse, 5′-AAA GCG GGT GAT CCA GAT G-3′; AP-1-4 forward, 5′-GGA GCG GAG GAA GGA GTC-3′; AP-1-4 reverse, 5′-GGC AAC GGA AAA GTC TCA AA-3′; AP-1-5 forward, 5′-GCC ACA GAT CCC CTA TTC AA-3′; AP-1-5 reverse, 5′-GTC TCC CGG CAA AAG GTA G-3′; 5′ distal forward, 5′-ATC CCG TGC TCA CTA TGC TC-3′; 5′ distal reverse, 5′-GAG TCC CAA GGC TAG TGT GC-3′; 3′ distal forward, 5′-TCG GAT TTG TGT GTT CAG GA-3′; and 3′ distal reverse, 5′-GCT GGG GAC ACA CAT AGA CA-3′. Although the amplicons are variable in size, the PCR efficiencies of these primers were comparable to each other, with similar titration slopes ranging from −3.0 to −3.5.

Nuclear extract preparation and NF-κB and AP-1 activation assays

Nuclear extracts from A549 cells were prepared using the Nuclear Extraction kit from Active Motif. NF-κB p65 and AP-1 c-Jun activation were measured with TransAM NF-κB p65 and AP-1 family kits (Active Motif) according to the manufacturer's instructions.

NF-κB and AP-1/TGF-β1 promoter binding assays

DNA oligonucleotides containing a putative NF-κB or AP-1 site and mutated oligonucleotides were prepared by mixing equal amounts of 100 μM sense and antisense oligonucleotides with annealing buffer (10 mM PBS (pH 7.5), 50 mM NaCl, 0.1% Tween 20, and 2.7 mM KCl), incubating in a preheated block (95°C), and leaving the culture at room temperature for 60 min. Streptavidin-coated microplates (Thermo Labsystems) were immobilized with 0.25 μM biotinylated DNA oligonucleotides in the TGF-β1 promoter in annealing buffer (10 mM Tris-HCl (pH 7.5), 50 mM NaCl, and 1 mM EDTA) overnight at 4°C. The binding reaction was performed by incubating nuclear extracts (20 μg/20 μl) from A549 cells with 30 μl of binding buffer (4 mM HEPES (pH 7.5), 120 mM KCl, 8% glycerol, 1% BSA, 2 mM DTT, and 10 μg/ml herring sperm DNA) for 1 h at room temperature in the DNA oligonucleotide-immobilized microplates. In competitive binding experiments, nonbiotinylated wild-type (0.2 or 2 μM) or mutated (2 μM) oligonucleotides were added to the 30-μl binding buffer. After washing with washing buffer, DNA oligonucleotide-bound protein was detected with anti-p65 (1/1000; Active Motif) or anti-phospho-c-Jun Abs (1/500; Active Motif) and an HRP-conjugated goat anti-rabbit secondary Ab (1/500; DakoCytomation) diluted in buffer (10 mM PBS (pH 7.5), 50 mM NaCl, and 0.1% Tween 20). The colorimetric reaction was performed with 100 μl of substrate reagent (R&D Systems Europe), stopped with 50 μl of stop solution (2 N H_2SO4), and measured at 450 nm with a reference wavelength of 550 nm. The oligonucleotides used in these studies were as follows: κB1 sense, 5′-agg ctg ggt TGG AAA CTC Tgg gac aga a-3′; κB1 antisense, 5′-ttc tgt ccc aga gtt tcc aac cca gcc t-3′; κB2 sense, 5′-agg agt ctg GTC CCC ACC Cat ccc tcc t-3′; κB2 antisense, 5′-agg agg gat ggg tgg gga cca gac tcc t-3′; wild-type (w) κB3 sense, 5′-ggg ggc agg GGG GAC GCC Ccg tcc ggg g-3′; wκB3 antisense, 5′-ccc cgg acg ggg cgt ccc ccc tgc ccc c-3′; mκB3 sense, 5′-ggg ggc agg GGG GAG CCC Ccg tcc ggg g-3′; mκB3 antisense, 5′-ccc cgg acg ggg gct ccc ccc tgc ccc c-3′; AP-1-1 sense, 5′-cct ggg gtc TCC AGT GAG Tat cag gga g-3′; AP-1-1 antisense, 5′-ctc cct gat act cac tgg aga ccc cag g-3′; AP-1-2 sense, 5′-cgt gga gtg CTG AGG GAC Tct gcc tcc a-3′; AP-1-2 antisense, 5′-tgg agg cag agt ccc tca gca ctc cac g-3′; wAP-1-3 sense, 5′-ggc tcc cct GTG TCT CAT Ccc ccg gat t-3′; wAP-1-3 antisense, 5′-aat ccg ggg gat gag aca cag ggg agc c-3′; mAP-1-3 sense, 5′-ggc tcc cct GTG TCT GTT Ccc ccg gat t-3′; mAP-1-3 antisense, 5′-aat ccg ggg gaa cag aca cag ggg agc c-3′; AP-1-4 sense, 5′-ccc cag agt CTG GGA CGA Gcc gcc gcc g-3′; AP-1-4 antisense, 5′-cgg cgg cgg ctc gtc tca gac tct ggg g-3′; AP-1-5 sense, 5′-ctc cct gag GAG CCT CAG Ctt tcc ctc g-3′; and AP-1-5 antisense, 5′-cga ggg aaa gct gag gct cct cag gga g-3′. Mutated bases are underlined.

ChIP assay

After stimulation, protein-DNA complexes were cross-linked by formaldehyde (1% final concentration). Cells were resuspended in 200 μl of SDS lysis buffer (50 mM Tris (pH 8.1), 1% SDS, 5 mM EDTA, and complete proteinase inhibitor mixture) and subjected to five cycles of sonication on ice with 10-s pulses. Sonicated samples were centrifuged to spin down cell debris, and the soluble chromatin solution was immunoprecipitated using Abs specific for p65, c-Jun (Santa Cruz Biotechnology), acetylated histone

H4, acetylated histone H3 (Upstate Biotechnology), or RNA polymerase II (RNA Pol II; Abcam). Protein-bound immunoprecipitated DNA was washed with LiCl wash buffer and 10 mM Tris and 1 mM EDTA (pH 8.0), and immune complexes were eluted by adding elution buffer (1% SDS and 0.1 M $NaHCO_3$), followed by incubation for 4 h at 65°C in 200 mM NaCl and 1% SDS to reverse cross-links and incubation for 1 h at 45°C with 70 μg/ml proteinase K (Sigma-Aldrich). DNA was extracted with phenol/chloroform, precipitated with ethanol/0.3 M NaHCOOH/20 μg glycogen, and resuspended in 100 μl of nuclease free water. QPCR was performed with 8 μl of DNA sample for quantification.

Statistics

Data points and values in the text and figure legends represent the mean ± SEM of at least three independent determinations taken from different cell preparations. Groups of data were compared using the Mann-Whitney *U* test. Statistical significance was set at $p < 0.05$.

Results

Effect of IL-1β on TGF-β1 release

Active TGF-β1 levels in the conditioned medium of cultured A549 cells treated with 10 ng/ml IL-1β were measured at variable times (0–72 h). IL-1β rapidly increased active TGF-β1 release by 2.3-fold (8.4 ± 2.4 vs 19.2 ± 4.6 pg/ml; $p < 0.01$) at 24 h (Fig. 1*A*). This increase was maintained at 48 h (6.6 ± 2.4 vs 15.3 ± 4.3 pg/ml; $p < 0.01$) and 72 h (7.5 ± 1.5 vs 14.5 ± 5.6 pg/ml; $p < 0.01$; Fig. 1*A*). The release of active TGF-β1 in response to IL-1β was also concentration dependent; a significant induction was achieved with IL-1β at 0.01 ng/ml ($p < 0.05$) and was maximal at 0.1 ng/ml ($p < 0.01$), above which release plateaued (Fig. 1*B*).

To confirm that the IL-1β induction of active TGF-β1 release involves TGF-β1 production rather than just release from preformed stores, Western blot analysis of whole cell lysates was performed. Using a specific TGF-β1 Ab, a marked 5-fold increase in the TGF-β1-immunoreactive band at 25 kDa was detected after 24 h of incubation with 10 ng/ml IL-1β (ratio, 5.4 ± 0.4; compared with control values, $p < 0.01$; Fig. 1*C*) and declined from 48 to 72 h (Fig. 1*C*). By contrast, unstimulated cells contained very low TGF-β1 immunoreactivity at every time point studied (24, 48, and 72 h). These results parallel the time course of IL-1β induction of active TGF-β1 release.

Effects of AS602868, SP600125, and actinomycin D on active TGF-β1 release stimulated by IL-1β

To determine the mechanism by which active TGF-β1 release is augmented by IL-1β, unacidified conditioned medium with or without 10 ng/ml IL-1β stimulation for 24 h after variable pharmacological inhibitors pretreatments were assayed for active TGF-β1 by ELISA. Although there was no effect on basal TGF-β1

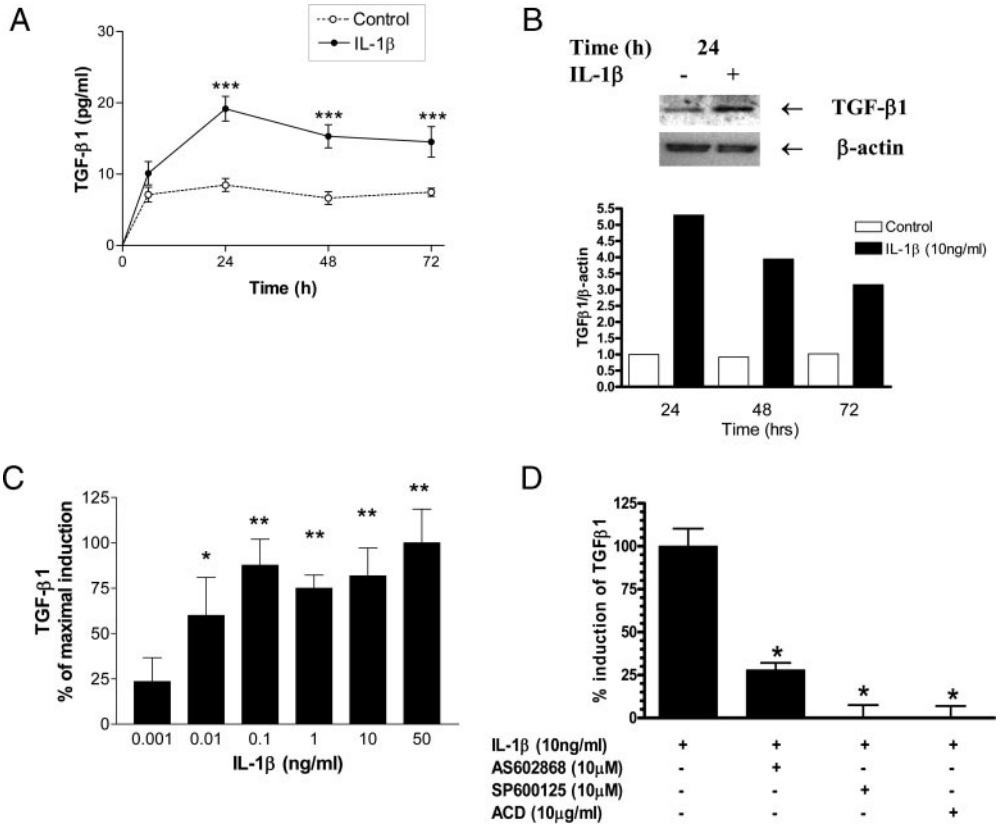

FIGURE 1. Effects of IL-1β on TGF-β1 protein production and release. *A*, Time course of IL-1β on TGF-β1 release. Cells were incubated with medium alone or IL-1β (10 ng/ml) for 0, 6, 24, 48, or 72 h. Supernatants were collected and assayed for active TGF-β1 by ELISA. *B*, Concentration-response curve of IL-1β on TGF-β1 release. Cells were incubated with various concentrations of IL-1β (0–50 ng/ml) for 24 h. Supernatants were collected and assayed for active TGF-β1 by ELISA. *, $p < 0.05$; **, $p < 0.01$ (vs nontreatment). Results are the mean ± the SEM, expressed as a percentage of maximal induction ($n = 3$ independent experiments). *C*, Effect of IL-1β on TGF-β1 protein production. Cells were incubated with medium alone or with IL-1β (10 ng/ml) for 24, 48, or 72 h. Protein extracts were obtained and examined for TGF-β1 by Western blotting (*upper panels*). Bar graphs (*lower panels*) show quantitative analysis of scanning densitometric values of TGF-β1 as a ratio to β-actin expression, which was used as a loading control. Data are examples of two or three independent experiments with similar results. *D*, Effects of AS602868, SP600125, and actinomycin D on IL-1β-stimulated active TGF-β1 release. Cells were pretreated with AS602868 (10 μM), SP600125 (10 μM), or actinomycin D (ACD; 10 μg/ml) for 1 h before incubation with medium alone or IL-1β (10 ng/ml) for 24 h. Supernatants were collected and assayed for active TGF-β1 by ELISA. *, $p < 0.05$ (vs IL-1β alone). Results are the mean ± SEM, expressed as the percent induction of TGF-β1 ($n = 3$ independent experiments).

release, the specific IKK2 inhibitor AS602868 (10 μM) inhibited IL-1β-induced active TGF-β1 release by 72% ($p < 0.05$, compared with IL-1β alone), whereas the specific JNK inhibitor, SP600125 (10 μM), and the transcription inhibitor, actinomycin D (10 μg/ml), completely abrogated this induction (Fig. 1*D*, and data not shown). These results suggest that the increases in the release of active TGF-β1 involve transcriptional processes and are related to NF-κB and JNK pathways.

IL-1β stimulates TGF-β1 mRNA expression

To investigate whether IL-1β stimulates TGF-β1 gene expression, we used real-time RT-QPCR to compare the levels of TGF-β1 mRNA in A549 cells with or without IL-1β stimulation at variable concentrations (0.1–10 ng/ml) for 6 h. Consistent with the basal secretion of TGF-β1 protein, constitutive expression of TGF-β1 mRNA was demonstrated (Fig. 2*A*). IL-1β caused an increase in the level of TGF-β1 mRNA in a concentration-dependent manner, with a maximal 1.7-fold induction ($p < 0.01$) achieved at 10 ng/ml (Fig. 2*A*).

The kinetics of TGF-β1 mRNA expression also demonstrated a time-dependent induction upon IL-1β (10 ng/ml) stimulation. Constitutive levels of TGF-β1 mRNA in control cells remain unchanged during 8 h of incubation, but revealed a slight increase (1.3-fold) after 24 h ($p < 0.05$; Fig. 2*B*). Upon IL-1β stimulation, the level of TGF-β1 mRNA increased 1.4-fold ($p < 0.05$) above baseline at 4 h, reached a maximum at 8 h (1.9-fold above baseline; $p < 0.01$), and was maintained at 24 h (1.7-fold above baseline; $p < 0.05$; Fig. 2B). This demonstrates that increases in active TGF-β1 release correlate with induction of TGF-β1 mRNA after IL-1β stimulation.

Effects of actinomycin D, AS602868, and SP600125 on IL-1β induction of TGF-β1 mRNA

To test whether NF-κB- and JNK-mediated TGF-β1 expression is regulated at the transcriptional level, actinomycin D (10 μg/ml), AS602868 (10 μM), and SP600125 (10 μM) were added 1 h before IL-1β (10 ng/ml) stimulation. Based on our initial time-course experiments, which revealed that the suppressive effect of AS602868 occurred earlier than that of SP600125, the study time points of 4 and 24 h were chosen. AS602868 completely prevented IL-1β induction of TGF-β1 mRNA at 4 h, whereas SP600125 had no effect at this time point (Fig. 2*C*); 24-h pretreatment with AS602868 or SP600125 partially inhibited the induction of TGF-β1 mRNA, whereas the combination of AS602868 and SP600125 markedly attenuated this induction to a level not significantly different from that seen with unstimulated cells (Fig. 2*D*). These data suggested that IKK2/NF-κB and JNK/AP-1 pathways collaboratively mediate the IL-1β-induced TGF-β1 gene expression, with NF-κB having an earlier effect than AP-1. Finally, pretreatment with actinomycin D (10 μg/ml) completely prevented the effect of IL-1β on TGF-β1 mRNA induction (Fig. 2*D*), confirming transcriptional involvement.

Effects of IL-1β on p65 NF-κB and c-Jun AP-1 activation

To determine activation of NF-κB and AP-1, we used TransAM NF-κB p65 and AP-1 family kits to measure the DNA binding activities of p65 and phospho-c-Jun in nuclear extracts from A549 cells stimulated with 10 ng/ml IL-1β for various times (0, 10, 20, 30, 60, 120, 180, and 240 min). We observed a rapid and strong induction of p65 activation upon stimulation with IL-1β (Fig. 3*A*). The induction appeared at 10 min (13.1-fold; $p < 0.05$), peaked at 20 min (26.8-fold; $p < 0.05$), and declined slightly at 180 min

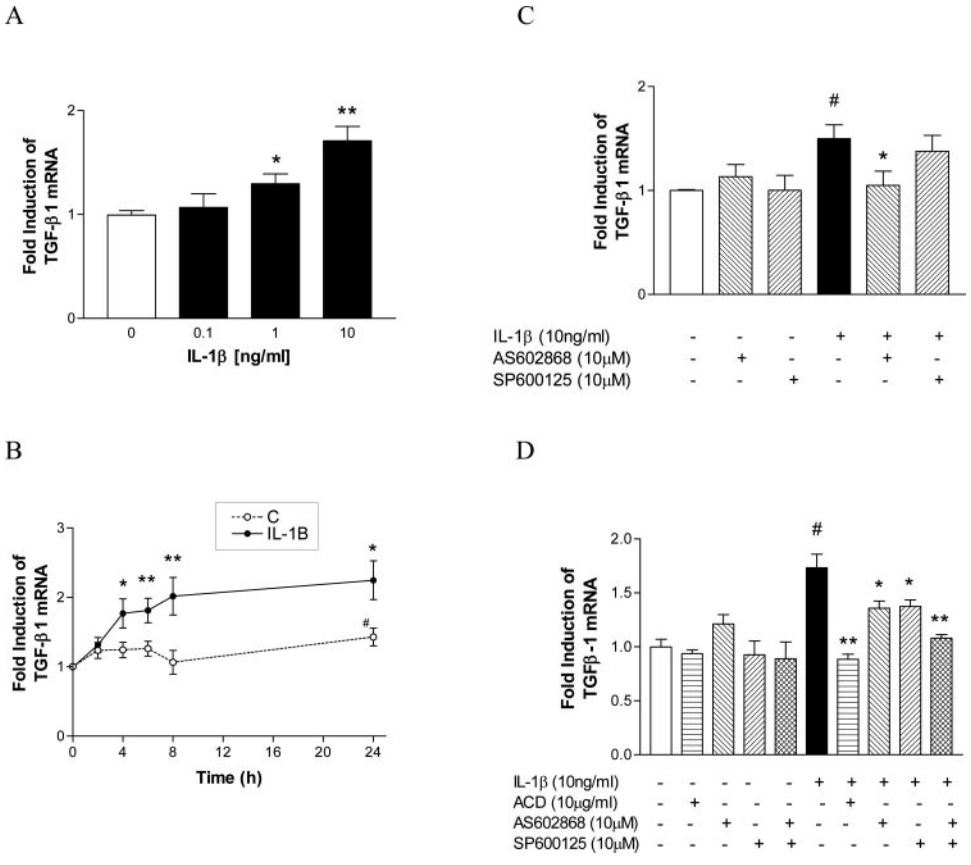

FIGURE 2. Effect of IL-1β on TGF-β1 mRNA induction. Cells were incubated with medium or IL-1β (0.1, 1, or 10 ng/ml) for 6 h (*A*) or IL-1β (10 ng/ml) for 0, 2, 4, 6, 8, or 24 h (*B*). Levels of TGF-β1 mRNA were quantified by real-time RT-QPCR and were normalized with respective GAPDH mRNA levels. *, $p < 0.05$; **, $p < 0.01$ (vs nontreatment). #, $p < 0.05$ (compared with time zero). Results are the mean ± SEM fold induction vs the medium control at time zero; at least three independent experiments were performed. *C* and *D*, Effects of actinomycin D, AS602868, and SP600125 on IL-1β-induced TGF-β1 gene expression. Cells were pretreated with actinomycin D (ACD; 10 μg/ml), AS602868 (10 μM), or SP600125 (10 μM) for 1 h before incubation with medium alone or with IL-1β (10 ng/ml) for 4 h (*C*) or 24 h (*D*). Levels of TGF-β1 mRNA were quantified by real-time RT-QPCR and were normalized with respective GAPDH mRNA levels. #, $p < 0.05$ (vs medium control). *, $p < 0.05$; **, $p < 0.01$ (vs IL-1β alone). Results are expressed as the mean ± SEM fold induction vs medium control; at least three independent experiments were performed.

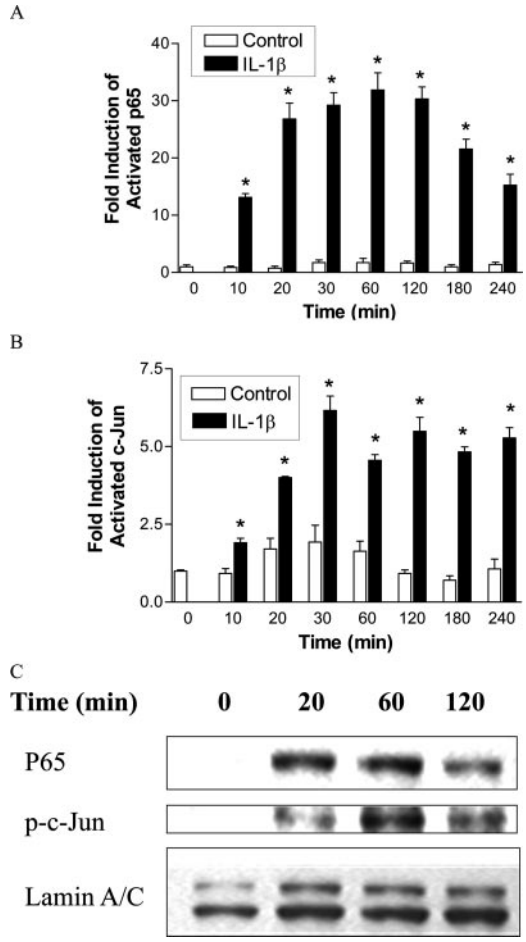

FIGURE 3. Effects of IL-1β on NF-κB and AP-1 activation. Cells were treated with IL-1β (10 ng/ml) or were left untreated for 0, 10, 20, 30, 60, 120, and 180 min. Nuclear extracts were assayed for NF-κB p65 (*A*) or AP-1 c-Jun (*B*) DNA binding activity using the TransAM NF-κB and AP-1 kits. *, $p < 0.05$ (vs nontreatment at time 0). Results are expressed as the mean $\pm$ SEM fold induction of $OD_{450\ nm}$ vs medium control at time zero; three independent experiments were performed. *C*, Effect of IL-1β on p65 and phospho-c-Jun nuclear expression. Cells were treated with IL-1β (10 ng/ml) for 0, 20, 60, and 180 min. Nuclear extracts were examined for p65 and phospho-c-Jun by Western blotting. Data are representative of two independent experiments with similar results.

(21.6-fold; $p < 0.05$) and 240 min (15.3-fold; $p < 0.05$; Fig. 3*A*). Similar to p65, the DNA binding activity of c-Jun rapidly increased at 10 min (1.9-fold; $p < 0.05$) after stimulation with IL-1β and peaked at 30 min (6.6-fold; $p < 0.05$), but remained elevated at 240 min (5.5-fold; $p < 0.05$; Fig. 3*B*). IL-1β-induced p65 and c-Jun activation was also confirmed by Western blotting with specific Abs against p65 and phospho-c-Jun (Fig. 3*C*), which showed nuclear expression of these activated transcription factors with very similar kinetics as those in TransAM experiments.

Selective recruitment of p65 and c-Jun to response elements in the native TGF-β1 promoter in vivo

To determine whether the roles of NF-κB and AP-1 pathways in the induction of TGF-β1 transcriptional activation, as noted above, are direct, we performed ChIP assays with Abs specific to p65 and c-Jun to measure the in vivo binding of p65 and c-Jun to the human TGF-β1 promoter. Analysis of the TGF-β1 promoter using AliBaba2.1 (⟨www.gene-regulation.com/pub/programs/alibaba2⟩) showed three putative NF-κB binding sites (κB1, −2105 to −2096; κB2, −2014 to −2005; κB3, −789 to −780, from the translation start site; Fig. 4) and five putative AP-1 binding sites (AP-1-1, −2054 to −2045; AP-1-2, −1660 to −1651; AP-1-3, −1211 to −1202; AP-1-4, −681 to −672; AP-1-5, −129 to −120, from the translation start site; Fig. 5, *A* and *B*). Primer pairs with QPCR products from 95 to 233 bp were designed to amplify the DNA corresponding to the above putative κB and AP-1 sites and were used to measure the DNA fragments in immunoprecipitates with real-time QPCR. As a negative control, a set of primers amplifying a distal site 3′ to the translation start site, 25665–25797 from the translation start site, were used. The time course of p65 ChIP showed that p65 was recruited to the κB3 site from 60–120 min after IL-1β stimulation, before declining at 180 and 240 min (Fig. 4*C*). In contrast, the amounts of DNA fragments with the κB1, κB2, and 3′-distal sites in the immunoprecipitates were similar and remained unchanged at all time points after IL-1β stimulation (Fig. 4*C*), suggesting no recruitment of p65 to these sites and specificity of the κB-3 site enrichment. The IL-1β-induced recruitment of p65 was prevented by pretreatment with AS602868 (10 μM; Fig. 4*D*), confirming that p65 was inhibited in the above-described parallel ELISA and real-time RT-QPCR experiments.

Surprisingly, c-Jun recruitment to the native TGF-β1 promoter occurred with markedly slower kinetics, being observed between 120 and 180 min after stimulation (Fig. 5*C*). This recruitment only occurred at the AP-1-3 site (Fig. 5*C*), whereas the associations of c-Jun to AP-1-1, AP-1-2, AP-1-4, AP-1-5, and the 3′ distal site were variable, with no significant difference from the basal levels (Fig. 5*C* and data not shown), suggesting the specificity of AP-1-3 site binding. Again, the recruitment of c-Jun to the AP-1-3 site was significantly abrogated by pretreatment with SP600125 (10 μM; Fig. 5*D*), confirming the effect of this compound. Taken together, these data demonstrate that p65 and c-Jun were recruited to the native TGF-β1 promoter and support the suggestion that p65 and c-Jun directly mediate the induction of TGF-β1 transcription upon IL-1β stimulation.

Binding of p65 and phospho-c-Jun to the κB3 and AP-1-3 sites in vitro

To confirm that the binding of p65 and phospho-c-Jun to the κB-3 and AP-1 sites are DNA sequence specific, we performed an ELISA-based DNA binding assay with nuclear extracts prepared from A549 cells. Using specific anti-p65 and anti-phospho-c-Jun Abs, this assay detected proteins binding to immobilized κB3 and AP-1-3 oligonucleotides (Fig. 6*A*), respectively. Upon stimulation with IL-1β (10 ng/ml), the binding activity of p65 to the κB3 oligonucleotide increased dramatically ($p < 0.01$; Fig. 6*B*). Addition of an excess of the free wκB3 oligonucleotides (wκB3) at 0.2 and 2 μM, but not the mκB3 oligonucleotides (mκB3; Fig. 6*B*), specifically competed this binding in a concentration-dependent manner ($p < 0.05$ and $p < 0.01$, respectively; Fig. 6*B*), suggesting the specificity of this p65 binding to the κB3 site. Similarly, IL-1β increased the binding activity of phospho-c-Jun to the AP-1-3 oligonucleotide ($p < 0.01$), which was inhibited by adding the free wAP-1-3 oligonucleotide at 0.2 μM ($p < 0.05$) and 2 μM ($p < 0.01$), but not the mAP-1-3 oligonucleotide (Fig. 6*C*). Taken together, these data demonstrate that IL-1β induces p65 and phospho-c-Jun binding to the κB3 and AP-1-3 sites, and that this binding is DNA sequence specific.

p65 and c-Jun bind to only the κB3 and AP-1-3 sites on the TGF-β1 promoter in vivo (Figs. 4*C* and 5*C*). Another important issue was to determine whether this is due to different intrinsic affinities of the different sites. To this end, we conducted additional in vitro binding studies with all the putative binding sites. The results demonstrate that the κB3 and AP-1-3 sites had strikingly

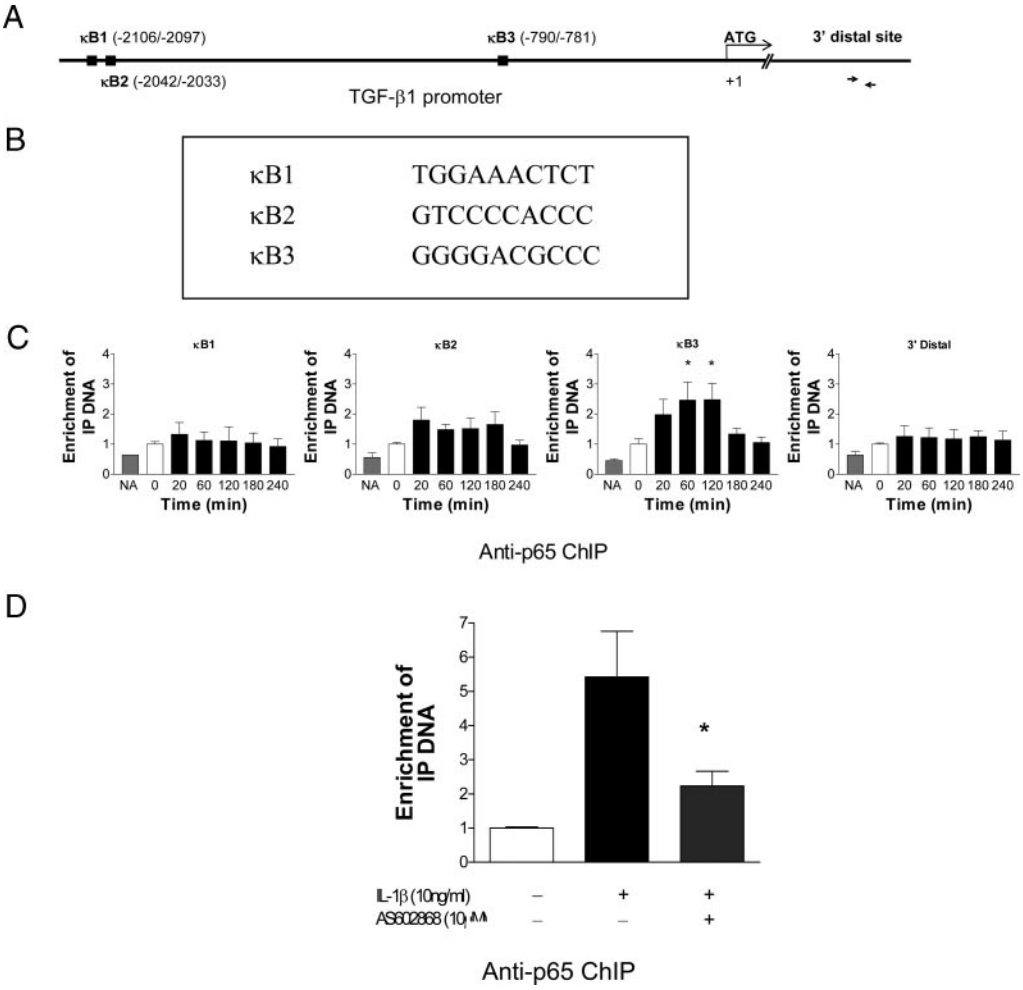

FIGURE 4. Effect of IL-1β on p65 recruitment to the TGF-β1 promoter. *A*, Schematic of the TGF-β1 promoter. The numbers indicate nucleotide positions in relation to the translation start site. Putative NF-κB binding sites (κB1, κB2, and κB3) and a distal site 3′ to the translation start site (3′ distal) are indicated. *B*, DNA sequences of putative NF-κB binding sites. *C*, Time course of p65 recruitment to the TGF-β1 promoter. Cells were incubated with IL-1β (10 ng/ml) for 0, 20, 60, 120, 180, or 240 min. p65 recruitment was determined by ChIP assay. The associated DNA was quantified by real-time QPCR with primer pairs specific for the putative κB sites (κB1, κB2, and κB3) and the 3′-distal sites. Values are normalized by input DNA. Results are expressed as the mean ± SEM fold induction vs basal levels. *, $p < 0.05$ (vs basal levels; $n = 3$ independent experiments). NA, no Ab control. *D*, Effect of AS602868 on p65 recruitment to the TGF-β1 promoter. Cells were pretreated with or without AS602868 (10 μM) for 1 h before IL-1β (10 ng/ml) stimulation for 60 min. p65 recruitment to the κB3 site was determined by ChIP assay. Values are normalized by input DNA. Results are expressed as the mean ± SEM fold induction vs basal levels. *, $p < 0.05$ (vs IL-1β alone; $n = 3$ independent experiments).

higher affinities for p65 and phospho-c-Jun than all other sites; the κB1 ($p < 0.001$) and κB2 sites ($p < 0.0001$) showed <14% the affinity for p65 as that seen with the κB3 site (Fig. 6*D*), whereas the AP-1-1 ($p < 0.01$), AP-1-2 ($p < 0.001$), AP-1-4 ($p < 0.01$), and AP-1-5 ($p < 0.001$) sites all showed <20% the affinity for the AP-1-3 site for phospho c-Jun (Fig. 6*E*). These results confirmed that only κB3 and AP-1-3 are sequence-specific p65 and c-Jun binding sites with high affinity in the TGF-β1 promoter.

NF-κB-mediated TGF-β1 transcription does not initiate from the common transcription start site

Two active promoters using two major transcription start sites, P1 and P2, have been reported for the TGF-β1 gene, with the first promoter activity located upstream to P1 and the second between P1 and P2 (15). The κB3 site is located between the P1 and P2 transcription start sites (Fig. 7*A*). We next asked whether NF-κB triggers this second promoter and leads to a smaller transcript than that transcribed from the P1 site. To this end, we designed a primer pair, TP1, amplifying a DNA sequence between P1 and P2 to examine the transcripts induced by IL-1β. As a positive control, we also designed another primer pair, TP2, to amplify a cDNA sequence in the same exon 1 in the coding sequence (CDS) of the human TGF-β1 gene (Fig. 7*A*). We chose 4 h as the observation time point, because by this time NF-κB is the major transcription factor mediating the IL-1β induction of TGF-β1 mRNA, as shown above. Interestingly, the induction of TGF-β1 mRNA was only observed with the TP2 ($p < 0.05$), not the TP1, primer pair (Fig. 7*B*). Furthermore, AS602868 (10 μM) abrogates the induction of the TGF-β1 mRNA detected with the TP2, but not the TP1, primer pair (Fig. 7*B*). Taken together, these data indicate that NF-κB triggers transcription of TGF-β1 from a start site downstream of P1, probably from P2, leading to a smaller transcript than that triggered by the P1 promoter.

Temporal effects on chromatin modifications and RNA Pol II recruitment to the native TGF-β1 promoter in vivo

We next asked whether the transcriptional induction of TGF-β1 is associated with acetylation of histones at the TGF-β1 promoter. To this end, additional ChIP assays were performed with Abs specific for acetylated histones H4 and H3. To determine whether histone

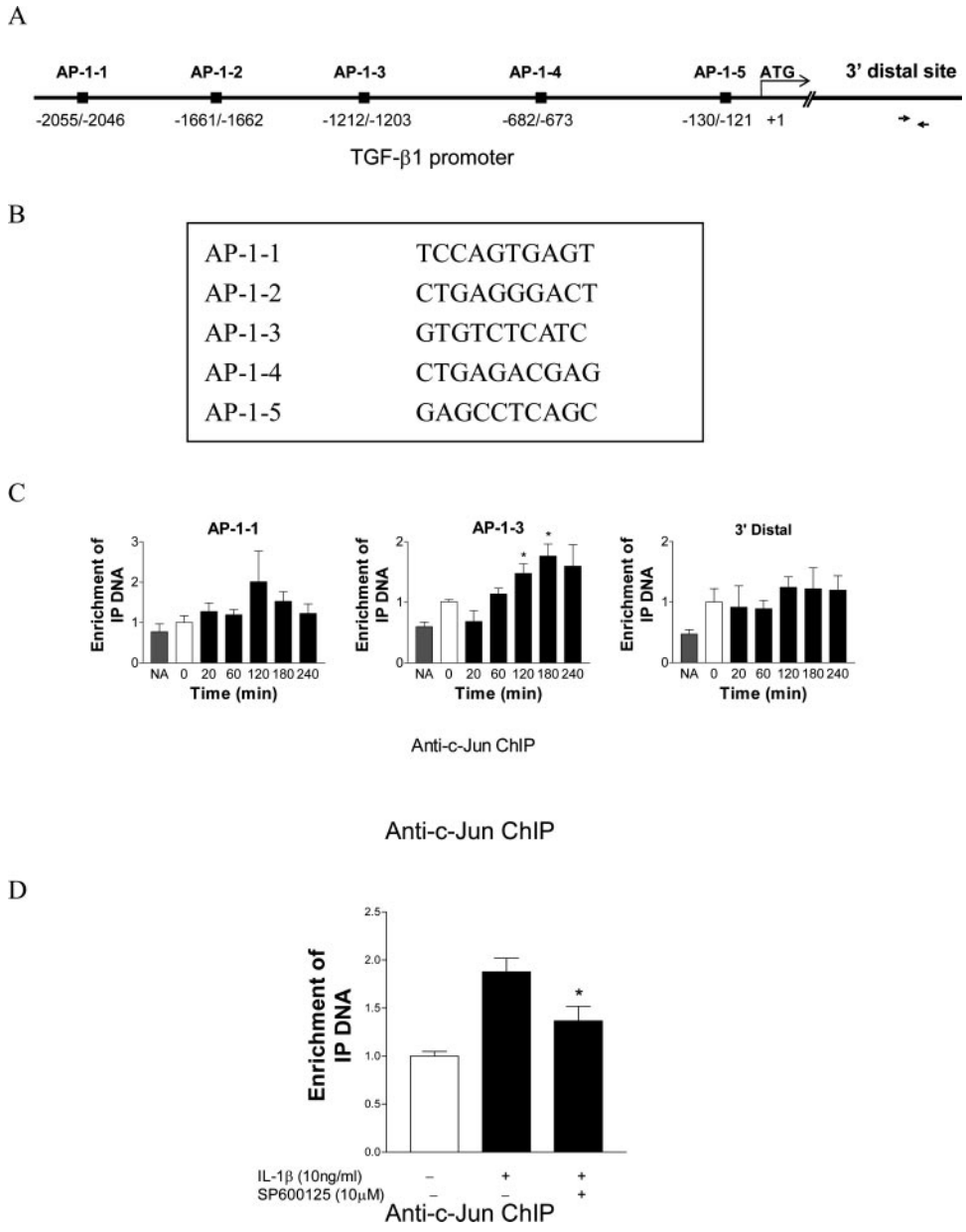

FIGURE 5. Effect of IL-1β on c-Jun recruitment to the TGF-β1 promoter. *A*, Schematic of the TGF-β1 promoter. The numbers indicate nucleotide positions in relation to the translation start site. Putative AP-1 binding sites (AP-1-1, AP-1-2, AP-1-3, AP-1-4, and AP-1-5) and the 3′-distal site are indicated. *B*, DNA sequences of putative AP-1 binding sites. *C*, Time course of c-Jun recruitment to the TGF-β1 promoter. Cells were incubated with IL-1β (10 ng/ml) for 0, 20, 60, 120, 180, or 240 min. c-Jun recruitment was determined by ChIP assay. The associated DNA was quantified by real-time QPCR with primer pairs specific for the putative AP-1 sites (AP-1-1, AP-1-2, AP-1-3, AP-1-4, and AP-1-5) and the 3′-distal site. Values are normalized by input DNA. Results are expressed as the mean ± SEM fold induction vs basal levels. *, $p < 0.05$ (vs basal levels; $n = 3$ independent experiments). NA, no Ab control. *D*, Effect of SP600125 on c-Jun recruitment to the TGF-β1 promoter. Cells were pretreated with or without SP600125 (10 μM) for 1 h before IL-1β (10 ng/ml) stimulation for 120 min. c-Jun recruitment to the AP-1-3 site was determined by ChIP assay. Values are normalized by input DNA. Results are expressed as the mean ± the SEM fold induction vs basal levels. *, $p < 0.05$ (vs IL-1β alone; $n = 3$ independent experiments).

acetylation changes are specific to transcription factor binding sites or continuous throughout the TGF-β1 promoter, four promoter regions, including a 5′-end site (the 5′ site), the in vivo p65 binding site (the κB3 site), the in vivo c-Jun binding site (the AP-1-3 site), and a region near the translation start site (the ATG site), were examined using primer pairs for the κB1 site, the AP-1-3 site, the κB3 site, and the AP-1-5 site, respectively (Fig. 8*A*). The results demonstrated an initial and maximal 1.7-fold increase in histone H4 acetylation at the κB3 site 60 min after IL-1β (10 ng/ml) treatment (Fig. 8*B*). Increases (1.5-fold) in histone H4 acetylation at this site persisted for the duration of experiment (240 min; Fig. 8*B*). Similar kinetics of histone H4 acetylation were observed at the promoter start site (the ATG site); it was increased by 1.6-fold at 60 min and maintained at 240 min. A constant acetylation level at the 5′-distal site indicated the specificity of the κB3 and ATG site enrichments. Interestingly, levels of histone H4 acetylation were unchanged at the 5′ site (Fig. 8*B*) and the AP-1-3 site (Fig. 8*B*). In sharp contrast with the early induction of histone H4 acetylation, increases in the levels of histone H3 acetylation were observed at later time points. These increases in histone H3 acetylation occurred at 120 min (1.2-fold) and peaked at 240 min (1.8-fold) at the κB3 site and, surprisingly, the 5′ site (1.9-fold at 120 min and 2.8-fold at 240 min; Fig. 8*C*). Again, the levels of histone H3 acetylation remained unchanged at the AP-1-3 and 3′-distal sites. Taken together, these data suggest that IL-1β induces histone H4 and H3 acetylations on distinct regions in the TGF-β1 promoter with different kinetics. It is speculated that histone H4 and H3 acetylations are differentially regulated and may play different roles in transcriptional activation of the TGF-β1 gene induced by IL-1β.

To assess the functional effect of histone acetylation on TGF-β1 expression, we inhibited deacetylation of histones using the histone deacetylase inhibitor TSA. Real-time RT-QPCR demonstrated that TSA (0, 1, 3, and 10 ng/ml) concentration-dependently augmented the levels of basal and IL-1β-induced TGF-β1 mRNA (Fig. 8*D*), suggesting that histone acetylation is critically involved in activation of the TGF-β1 gene.

RNA Pol II controls the synthesis of mRNA in eukaryotic cells. ChIP assays were also performed to examine the kinetics of RNA Pol II recruitment to the TGF-β1 promoter. As a negative control,

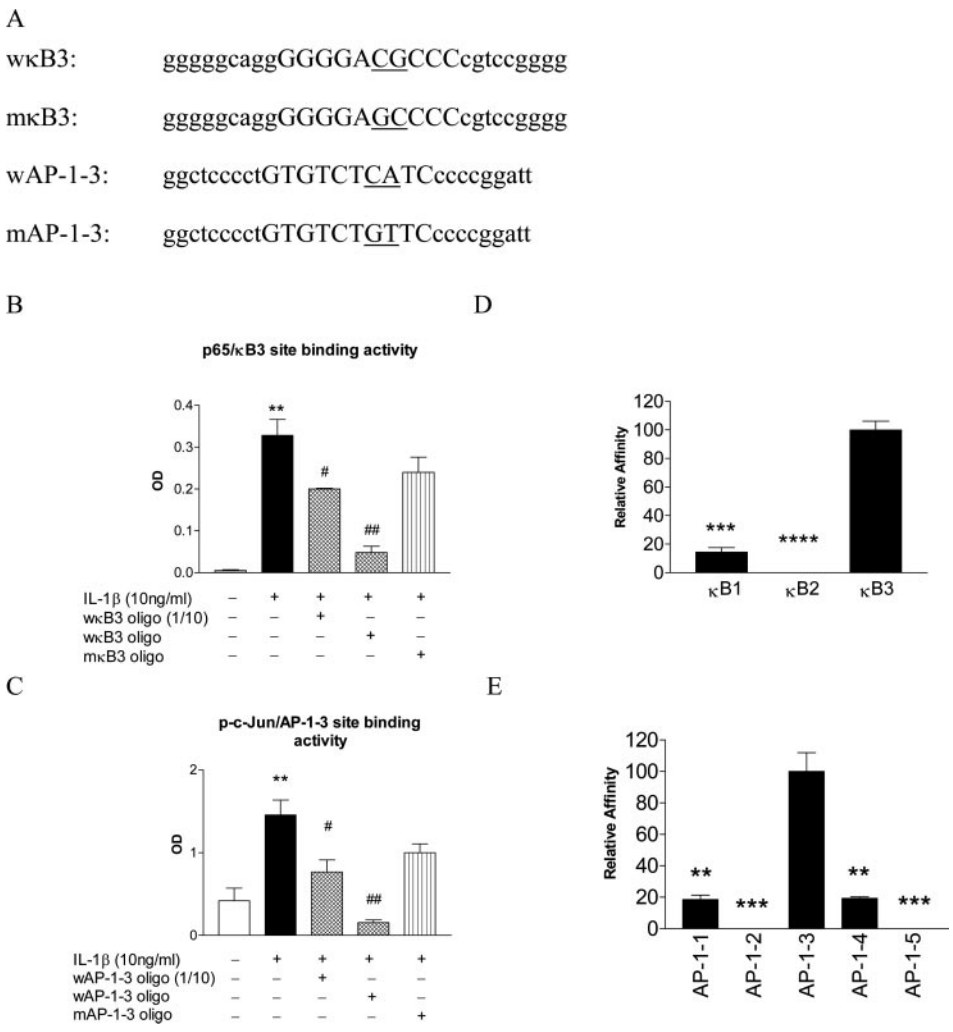

FIGURE 6. Binding of p65 and phospho-c-Jun to the DNA sequences in the TGF-β1 promoter in vivo. *A*, Sequences of the DNA oligonucleotides, including the κB3 and AP-1-3 sites or mutated oligonucleotides used in the NF-κB and AP-1/TGF-β1 promoter binding assays (only sense oligonucleotide sequences are shown). NF-κB or AP-1 binding sites are given in upper case, and mutations are underlined. Cells were treated with 10 ng/ml IL-1β for 1 h or were left untreated. Nuclear extracts were incubated with or without competitor DNA oligonucleotides (wκB3, wκB3 oligonucleotide; mκB3, mκB3 oligonucleotide; wAP-1-3, wAP-1-3 oligonucleotide; mAP-1-3, mAP-1-3 oligonucleotide) in 96-well plates immobilized with wκB3 (*B*) or wAP-1-3 (*C*) oligonucleotides and were detected by p65 or phospho-c-Jun specific Abs, respectively. Results are expressed as the mean ± SEM $OD_{450\ nm}$. *, $p < 0.05$; **, $p < 0.01$ (vs nontreatment). #, $p < 0.05$; ###, $p < 0.0001$ (vs IL-1β alone; $n = 3$ independent experiments). Affinities of the κB (*D*) and AP-1 (*E*) sites for p65 and phospho-c-Jun. Nuclear extracts from 10 ng/ml IL-1β-treated cells were incubated in 96-well plates immobilized with the κBs and AP-1s oligonucleotides as indicated and were detected with p65- or phospho-c-Jun-specific Abs. Results are expressed as the mean ± SEM of relative OD450. The data for κB3 and AP-1-3 are set at 100%. **, $p < 0.01$; ***, $p < 0.001$; ****, $p < 0.0001$ (vs κB or AP-1-3).

a primer pair amplifying a DNA region 5.5 kb upstream of the translation start site (−5517 to −5375 from the translation start site), the 5′-distal site, was also used. Without treatment, RNA Pol II was present along the TGF-β1 promoter (16.5 ± 5.5-, 89.3 ± 36.6-, and 47.0 ± 23.2-fold above the no Ab control level at the AP-1-3, κB3, and ATG sites, respectively; $p < 0.05$ at each site compared with 4.0 ± 0.9-fold at the 5′-distal site; Fig. 8*E*), consistent with the constitutive expression of this gene (Fig. 8*E*). Upon IL-1β stimulation, increased association of RNA Pol II was detected at all promoter regions under study (Fig. 8*E*; 5′, AP-1-3, κB3, and ATG sites). By contrast, RNA Pol II at the 5′-distal site remained unchanged during the study times, suggesting that the recruitment of RNA Pol II to the TGF-β1 promoter is region specific. Interestingly, maximal RNA Pol II recruitment to the region around the translation start site (1.8-fold; Fig. 8*E*; ATG site) coincided with the appearance of the first TGF-β1 transcripts (1.8-fold; Fig. 2*B*); both had similar levels of induction at 4 h. At the κB3 site, increases in RNA Pol II occurred at 120 min (Fig. 8*E*; κB-3 site), after p65 recruitment (Fig. 4*C*; κB3 site, 60 min), supporting the functional role of p65 in TGF-β1 transcription. Although a gradual increase in RNA Pol II binding at the AP-1-3 site was detected at early time points (Fig. 8*E*; AP-1-3 site; 20 and 60 min), at which time c-Jun recruitment could not be detected (Fig. 5*C*; AP-1-3 site), no concomitant induction of RNA Pol II was observed at the translation start site (Fig. 8*E*; ATG site; 20 and 60 min), suggesting that this RNA Pol II did not read through the promoter and was not functioning efficiently. Another significant rise in RNA Pol II binding at this site was seen at 240 min (Fig. 8*E*; AP-1-3 site), after the peak of c-Jun recruitment to the same region (Fig. 5*C*; AP-1-3 site). Furthermore, pretreatment with SP600125 (10 μM) inhibited the binding of RNA Pol II at 180 min, but had no effect on that at 120 min (data not shown), suggesting that RNA Pol II recruitment after 120 min was c-Jun dependent. Importantly, at all promoter regions at which histone acetylation changes were observed, RNA Pol II recruitment either occurred after histone H4 acetylation (Fig. 8, *B* and *E*; κB3 and ATG sites) or coincided with histone H3 acetylation (Fig. 8, *C* and *E*; 5′ and κB3 sites). Taken together, these results suggest that recruitment of p65 and c-Jun and histone modifications play important roles in recruitment of RNA Pol II, leading to transactivation of the TGF-β1 gene.

Discussion

The present study demonstrates that IL-β induces TGF-β1 protein and mRNA production from a human alveolar epithelial cell line. This induction involves de novo gene transcription and is mediated by NF-κB and AP-1. Using ChIP assays, we showed that p65 NF-κB and c-Jun AP-1 transcription factors were recruited to a novel NF-κB binding site and a reported AP-1 binding site in the TGF-β1 promoter upon IL-1β stimulation. Finally, IL-1β was shown to increase histone H4 and H3 acetylation at distinct regions of the TGF-β1 promoter, suggesting that hyperacetylation of histone H4 and H3 is associated with activation of the TGF-β1 gene.

The data in the present report demonstrate that NF-κB and AP-1 mediate the IL-1β induction of TGF-β1 gene expression. First,

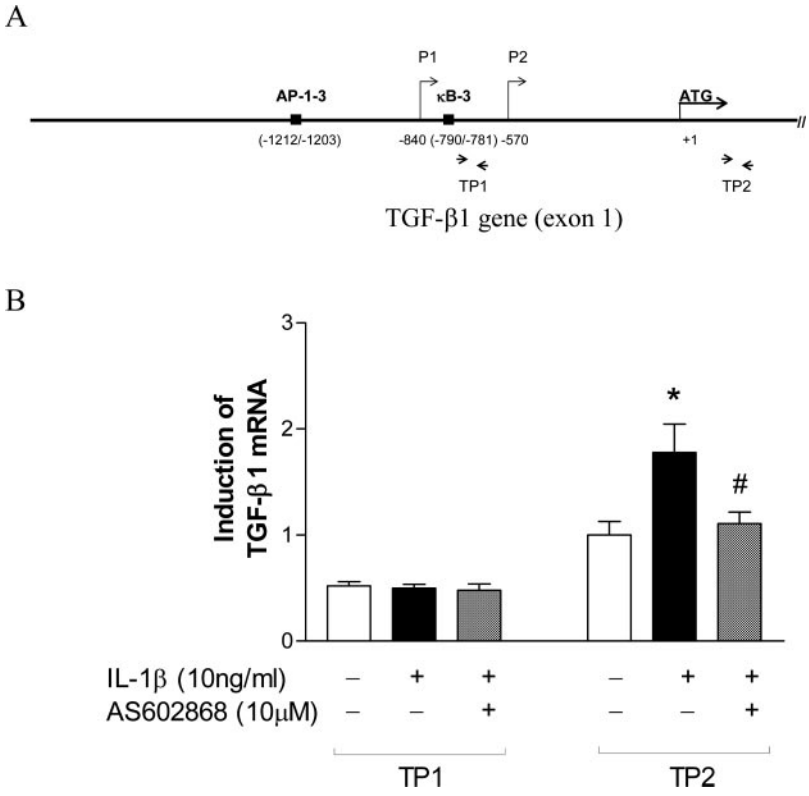

FIGURE 7. NF-κB does not use the first major transcription start site for inducing TGF-β1 transcription. *A*, Schematic illustration of exon 1 of the human TGF-β1 gene, in which the TGF-β1 promoter and the 5′ end of the CDS are included. The locations of the κB3 and AP-1-3 sites and the two major transcription initiation sites (P1 and P2) described by Kim et al. (15) are indicated. The DNA segments amplified by PCR primer pairs TP1 (between P1 and P2) and TP2 (in CDS) are also shown. The numbers indicate nucleotide positions in relation to the translation start site. *B*, TGF-β1 transcripts triggered by NF-κB. Cells were pretreated with or without AS602868 (10 μM) for 60 min before 10 ng/ml IL-1β stimulation for 4 h. TGF-β1 transcripts were determined by real-time RT-QPCR with TP1 or TP2 primer pairs as indicated in *A* and were normalized with respective GAPDH mRNA levels. *, $p < 0.05$ (vs not treated). #, $p < 0.05$ (vs IL-1β alone). Results are expressed as the mean ± SEM fold induction vs medium control examined by TP2 primers; at least three independent experiments were performed.

pretreatment of cells with selective IKK2 or JNK inhibitors partially inhibited the induction of TGF-β1 mRNA by IL-1β, which was completely abrogated by the combination of IKK-2 and JNK inhibitors. Second, using ChIP assays, p65 NF-κB and c-Jun AP-1 were bound to distinct sites in the TGF-β1 promoter in vivo. The sizes of the amplicons selected for the QPCR analyses range from 95–233 bp and were selected to match the potential κB and AP-1 sites. The small size of the amplicons allowed discrimination between chromatin at a resolution limited only by the size of the chromatin fragments after sonication, which is, on the average, 500 bp (26, 27). In theory, this arrangement will discriminate between the κB and AP-1 sites in the TGF-β1 promoter, except between the κB1 and κB2 sites, which are 64 bp apart and showed no increase in binding (Figs. 4, *top left panel*, and 5*A*). Furthermore, the increased binding of p65 and c-Jun was specific, because two of the three potential NF-κB sites and four of the five potential AP-1 sites in the TGF-β1 promoter did not increase transcription factor recruitment. Third, with NF-κB and AP-1/TGF-β1 promoter binding assays, we provided evidence that the κB3 and the AP-1-3 sties are sequence-specific p65 and c-Jun binding sites upon IL-1β stimulation. Finally, RNA Pol II was shown to be recruited to the κB3 and AP-1-3 sites temporally, consistent with the recruitment of p65 and c-Jun. Taken together, these data suggest that NF-κB and AP-1 are intimately involved in the transcriptional activation of TGF-β1.

The observation that NF-κB mediates TGF-β1 gene expression is in accordance with previous reports. In the embryonic chick lung, hyperactivation of NF-κB by the expression of IKK50, a constitutively active isoform of human IKK2, resulted in intense mesenchymal TGF-β1 expression (28). Treatment with RelA antisense oligonucleotides inhibited TGF-β1 mRNA expression in fibrosarcoma cells (19) and in monocytes from patients with idiopathic myelofibrosis (18). Nevertheless, none of these reports demonstrated a direct role of NF-κB in transcriptional activation of the TGF-β1 gene. The present study for the first time provides evidence that NF-κB is bound to the TGF-β1 promoter in intact cells and in vitro on a specific NF-κB binding site and mediates the induction of TGF-β1 transcription. This observation is contrary to the speculation by Perez et al. (19). Based on the finding that treatment with RelA antisense oligomers failed to inhibit TGF-β1 promoter-driven chloramphenicol acetyltransferase activity, Perez et al. (19) argued that the effect of RelA on TGF-β1 mRNA could be post-transcriptional. Indeed, two active promoters have been reported (15) for the TGF-β1 gene (Fig. 7*A*). The TGF-β1-chloramphenicol acetyltransferase reporter construct used in the experiments by Perez et al. (19), PHTG-2, includes only the first promoter, whereas the unique NF-κB binding site, the κB3 site, discovered in the present study is 5′ to the second promoter. In accordance with this, ChIP assay experiments failed to reveal increased recruitment of p65 to the other two potential NF-κB binding sites in the P1 promoter. However, the data in this study cannot exclude direct binding of p65 or other NF-κB family proteins to the first promoter of TGF-β1 in situations other than after IL-1β stimulation.

The present data also suggest that AP-1 is involved in the IL-1β induction of TGF-β1 transcription. The AP-1-3 site found in this study is also responsible for phorbol ester responsiveness, TGF-β1 autoinduction (16), and hyperglycemia-induced activation of the human TGF-β1 gene (29) in reporter assay systems. The present study also demonstrates binding of c-Jun protein to this site in the native promoter in vivo. The observation that pretreatment with IKK2 inhibitor or JNK inhibitor only partially blocked the induction of TGF-β1 mRNA, whereas the combination of both inhibitors completely abolished this induction, suggests that full responsiveness to IL-1β required cooperation between regulatory elements in both TGF-β1 promoters.

The data in this study also suggest a role for histone acetylation in TGF-β1 induction. ChIP assays demonstrated a time-dependent induction of histone H4 and H3 acetylation on the TGF-β1 promoter upon IL-1β stimulation. In addition, inhibition of HDAC

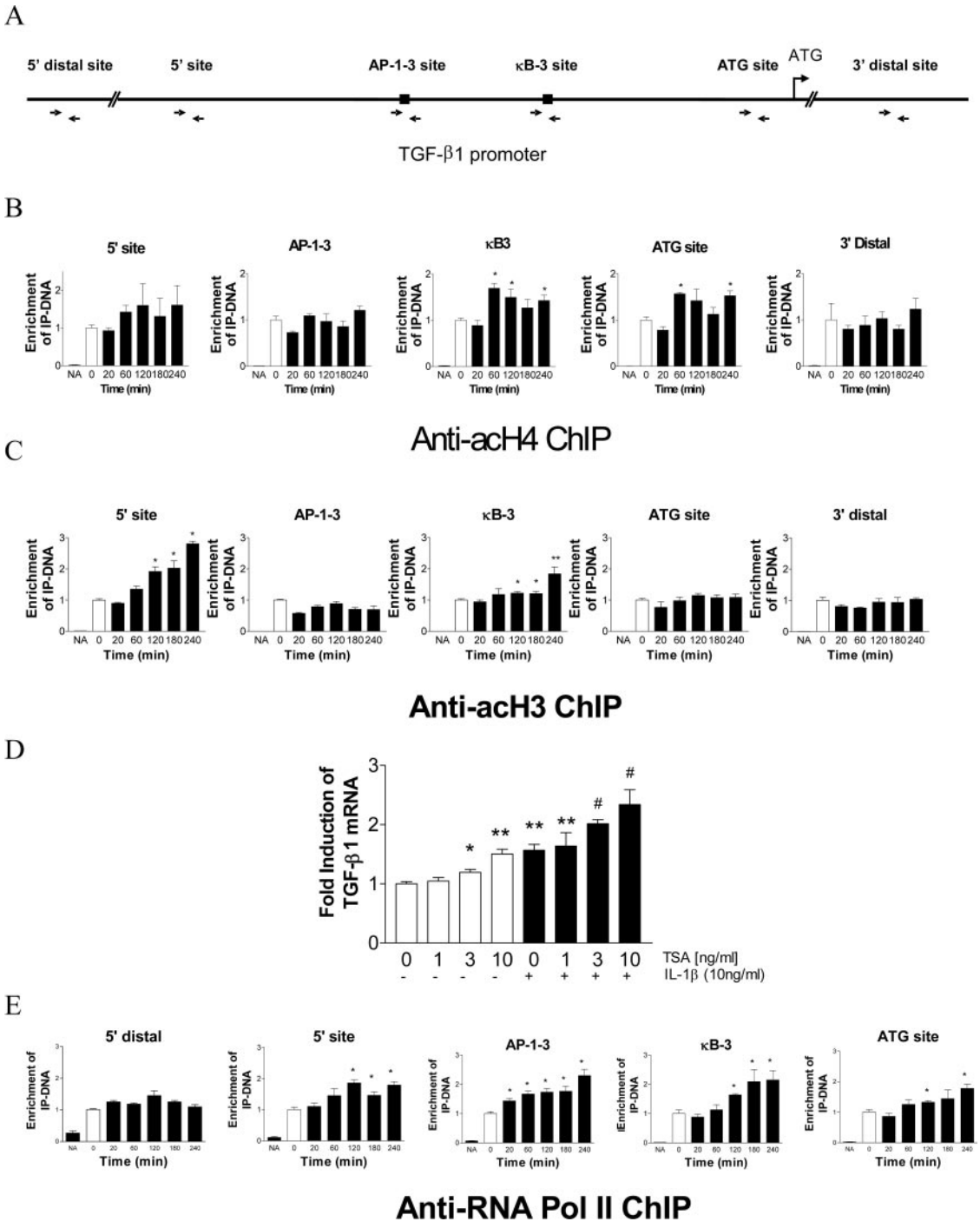

FIGURE 8. Effect of IL-1β on histone H4 and H3 acetylation and recruitment of RNA Pol II to the TGF-β1 promoter. *A*, Schematic of the TGF-β1 promoter. The DNA segments amplified by PCR primer pairs are indicated. *B* and *C*, Time course of histone acetylation on the TGF-β1 promoter. Cells were incubated with IL-1β (10 ng/ml) for 0, 20, 60, 120, 180, or 240 min. The acetylated status of histones H4 (*B*) and H3 (*C*) was determined by ChIP assay. The associated DNA was quantified by real-time QPCR with primer pairs specific for distinct TGF-β1 promoter regions, as indicated in *A*. Values are normalized by input DNA. Results are expressed as the mean ± SEM fold induction vs basal levels. *, $p < 0.05$; **, $p < 0.01$ (vs basal levels; $n = 3$ independent experiments). NA, no Ab control. *D*, Effect of TSA on TGF-β1 mRNA expression. Cells were pretreated with 0, 1, 3, and 10 ng/ml TSA for 30 min before 10 ng/ml IL-1β stimulation for 6 h. Levels of TGF-β1 mRNA were quantified by real-time RT-QPCR and were normalized with respective GAPDH mRNA levels. acH3, acetylated histone 3. *, $p < 0.05$; **, $p < 0.01$ (vs not treated). #, $p < 0.05$ (vs IL-1β alone). Results are expressed as the mean ± SEM fold induction vs medium control; at least three independent experiments were performed. *E*, Time course of RNA Pol II recruitment to the TGF-β1 promoter. Cells were incubated with IL-1β (10 ng/ml) for 0, 20, 60, 120, 180, or 240 min. The association of RNA Pol II with TGF-β1 promoter was determined by ChIP assay as indicated in *B* and *C*. Results are expressed as the mean ± SEM fold induction vs basal levels. *, $p < 0.05$ (vs basal levels; $n = 3$ independent experiments). NA, no Ab control.

activities with TSA was shown to enhance both basal and IL-1β-induced TGF-β1 transcription. The kinetics of RNA Pol II recruitment that followed histone H4 acetylation and/or coincided with histone H3 acetylation provided additional support that histone acetylation is critically implicated in transactivation of the TGF-β1 gene. In the four promoter regions examined, relatively high

variable basal levels of acetylated histones H4 and H3 were demonstrated, consistent with the constitutive expression of the gene. IL-1β-induced hyperacetylated histones H4 and H3 mainly occurred on the κB3 site, suggesting that these histone modifications might be related to the recruitment of NF-κB. NF-κB p65 binding is required for the acetylation of histones H3 and H4 at the proximal promoter region and the TNF responsive element in the murine manganese superoxide dismutase gene after TNF-α stimulation (30). In contrast, recruitment of NF-κB to the promoters of the genes with regulated and late accessibility required hyperacetylation of histone H4 in murine macrophages stimulated with LPS (31). In the present study, recruitment of p65 appears to occur before increases in histone H4 and H3 acetylation. Our data also revealed that increases in histone H4 acetylation occurred around the translation start site (the ATG site) with a pattern similar to that around the κB3 site. Given that the two sites are 660 bp apart, which is roughly equal to four or five nucleosomes, and that no histone H4 acetylation change was detected at a site 422 bp upstream to the κB3 site, the AP-1-3 site, these data suggest that NF-κB-associated histone H4 acetylation either affected more than one nucleosome or spread further downstream, possibly due to HAT activities accompanying elongating RNA Pol II (32, 33).

Unexpectedly, we observed an increase in histone H3 acetylation at a far distal site, the 5′ site. This chromatin modification was associated with augmented recruitment of RNA Pol II, suggesting that hyperacetylation of histone H3 at this site is also associated with TGF-β1 transactivation. It is likely that this H3 hyperacetylation is NF-κB-related through a three-dimensional contact with the κB-3 site. Alternatively, it may be mediated by an as yet unidentified DNA binding factor. By contrast, the acetylation status of histones H4 and H3 on the AP-1-3 site was unchanged, although an additional increase in RNA Pol II did occur after c-Jun binding. However, the mechanism responsible for the initial induction of RNA Pol II recruitment to the AP-1-3 site before c-Jun occupancy is not clear. Increased intrinsic accessibility or affinity of this site for phospho-c-Jun or RNA Pol II may account for these effects before histone acetylation occurs. Delineation of the chromatin structure in this region will be required to confirm this. It has been reported that p38 MAPK-mediated histone H3 phosphorylation enhances binding of RNA Pol II to MKP-1 chromatin (34). Nevertheless, the specific p38 inhibitor, SB203580, had no effect on TGF-β1 mRNA induction, and an increase in histone H3 phosphorylation was not observed at corresponding times (data not shown). Other histone modifications, e.g., histone methylation, may play a role in this RNA Pol II recruitment.

Taken together, these data suggested that IL-1β induces histone H4 and H3 acetylation on distinct regions of the TGF-β1 promoter, which is required for RNA Pol II recruitment, leading to the transactivation of the TGF-β1 gene. This acetylation is either not associated with c-Jun recruitment or involved recruitment of chromatin remodeling factors through bromodomain interactions (20) allowing transcription factor DNA association at distal sites. Additional studies examining modifications (acetylation and/or methylation) of individual H3 and H4 residues throughout the TGF-β1 promoter during this time frame may reveal a greater association with TGF-β1 gene induction.

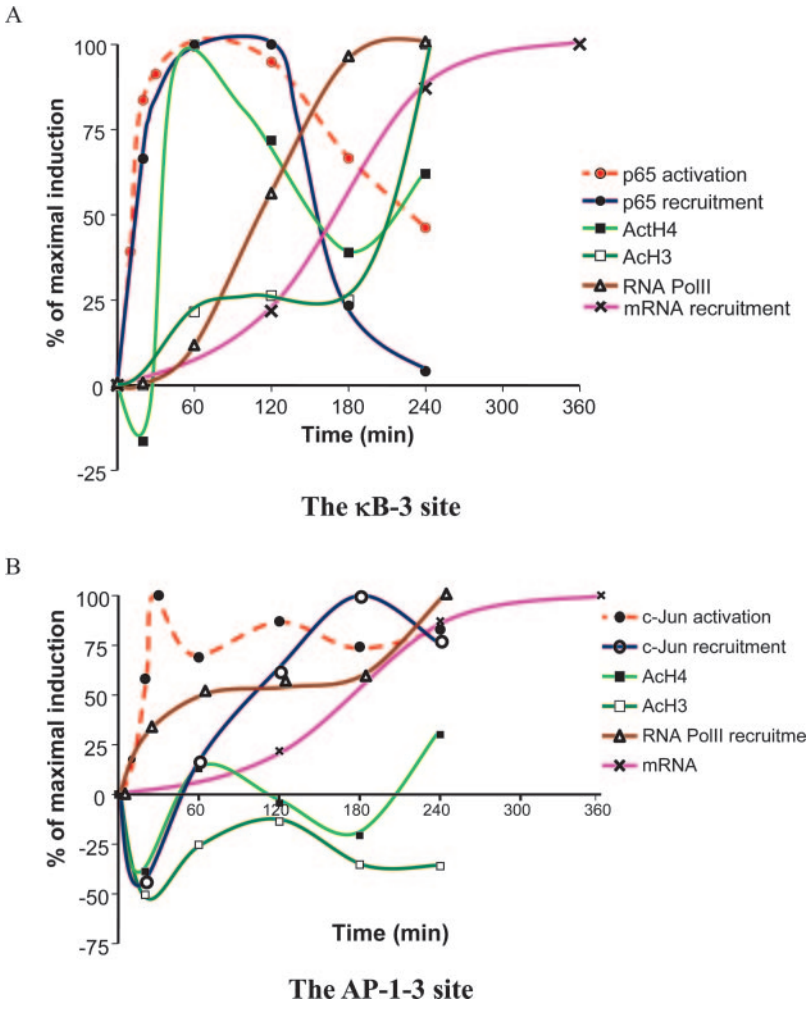

FIGURE 9. Kinetics of signal activation, transcription factor recruitment, histone acetylation, and RNA Pol II recruitment in TGF-β1 gene activation. The time courses of p65 and c-Jun activation and the events that occurred on the κB3 site (*A*) and the AP-1-3 site (*B*) in the TGF-β1 promoter are summarized. Mean enrichment minus mean background (resting cell values) were calculated and expressed as a percentage of the maximal values. Experimental variations are shown in Figs. 2–6. Data for acetylated histones (ActH3 and ActH4) at the AP-1-3 site are compared with the maximal enrichment seen at the κB3 site. The sequential events of p65 and c-Jun transcription factor activation and recruitment, histone acetylation, and RNA Pol II recruitment on the TGF-β1 promoter result in transcription of the human TGF-β1 gene.

Our results demonstrate that transcription activation of the TGF-β1 gene by IL-1β depends on the ordered coordination of transcription factor activation and recruitment of transcription factors and histone acetylation on the TGF-β1 promoter (see Fig. 9). Induction of the TGF-β1 gene first triggers activation of the NF-κB and AP-1 pathways (Fig. 9), rapidly followed by recruitment of p65 and histone H4 hyperacetylation at the κB3 site, at which histone H3 hyperacetylation and RNA Pol II recruitment followed as later events (Fig. 9*A*). At the AP-1-3 site, recruitment of c-Jun was followed by an increase in RNA Pol II recruitment (Fig. 9*B*). All these events occurring at the promoter culminated in the transcription of TGF-β1 mRNA. Compared with the rapid activation, the recruitment of c-Jun to promoter appears to be slower; the peak of c-Jun recruitment was delayed for 150 min after activation, suggesting that the AP-1-3 site is not accessible at an early time of induction. It has been reported that c-Jun/c-Fos-induced chromatin remodeling activity increased 10-fold on an acetylated nucleosome template, suggesting that there is an inherent connection among chromatin remodeling, regulator recruitment, and histone modification (35). In this study we did not find any increase in histone H4 or H3 acetylation on the AP-1-3 site, suggesting that histone acetylation is not involved in regulating the accessibility of this region. Additional studies must be conducted to explore whether other chromatin modifications or remodeling factors are implicated in the recruitment of c-Jun to this site.

The stimulation of total TGF-β1 release by IL-1β has been described previously in numerous cells types, including peritoneal mesothelial cells (14), endothelial cells (13), and smooth muscle cells (36). The present data also show that IL-1β increases not only total TGF-β1, but also active TGF-β1, release from A549 cells. This observation supports the concept that lung epithelial cells may be actively involved in the fibrotic or remodeling process of chronic inflammatory lung diseases. The mechanism by which IL-1β enhances active TGF-β1 release may be independent, at least partially, of production through a transcriptional process. Western blotting revealing that intracellular TGF-β1 was increased, and IL-1β-increased TGF-β1 mRNA was abrogated by actinomycin D; both of these findings support TGF-β1 production through de novo gene transcription. However, the concentrations of IL-1β required to stimulate TGF-β1 mRNA and active TGF-β1 release were different. Given the facts that increases in TGF-β expression do not always correlate with increases in active TGF-β release (37) and that the major regulatory step controlling TGF-β1 activity takes place extracellularly (38), it is tempting to speculate that in addition to transcriptionally active TGF-β1 expression, IL-1β has impact on activation of the protein. A variety of molecules, including plasmin (39), thrombospondin-1 (40), and integrins (41), have been described as latent TGF-β1 activators. Additional studies need to be undertaken to explore the mechanism by which TGF-β1 is activated by IL-1β.

In conclusion, we have demonstrated that, similar to proinflammatory cytokines, the transcription of TGF-β1 is activated by NF-κB and AP-1 upon IL-1β stimulation. This activation is triggered by direct recruitment of NF-κB and AP-1 transcription factors to the corresponding binding sites in the TGF-β1 promoter, followed by NF-κB-related histone H4 and H3 acetylation and recruitment of RNA Pol II, leading to the transcription of TGF-β1. The mechanism by which histone hyperacetylation is controlled and the roles of other histone modifications in the induction of TGF-β1 gene remain to be investigated.

Disclosures

The authors have no financial conflict of interest.

References

1. Massague, J. 1990. The transforming growth factor-β family. *Annu. Rev. Cell Biol.* 6: 597–641.
2. Sporn, M. B., A. B. Roberts, L. M. Wakefield, and R. K. Assoian. 1986. Transforming growth factor-β: biological function and chemical structure. *Science* 233: 532–534.
3. Border, W. A., and N. A. Noble. 1994. Transforming growth factor β in tissue fibrosis. *N. Engl. J. Med.* 331: 1286–1292.
4. de Boer, W. I., A. van Schadewijk, J. K. Sont, H. S. Sharma, J. Stolk, P. S. Hiemstra, and J. H. van Krieken. 1998. Transforming growth factor β1 and recruitment of macrophages and mast cells in airways in chronic obstructive pulmonary disease. *Am. J. Respir. Crit. Care Med.* 158: 1951–1957.
5. Takizawa, H., M. Tanaka, K. Takami, T. Ohtoshi, K. Ito, M. Satoh, Y. Okada, F. Yamasawa, K. Nakahara, and A. Umeda. 2001. Increased expression of transforming growth factor-β1 in small airway epithelium from tobacco smokers and patients with chronic obstructive pulmonary disease (COPD). *Am. J. Respir. Crit. Care Med.* 163: 1476–1483.
6. Redington, A. E., J. Madden, A. J. Frew, R. Djukanovic, W. R. Roche, S. T. Holgate, and P. H. Howarth. 1997. Transforming growth factor-β1 in asthma: measurement in bronchoalveolar lavage fluid. *Am. J. Respir. Crit. Care Med.* 156: 642647.
7. Minshall, E. M., D. Y. Leung, R. J. Martin, Y. L. Song, L. Cameron, P. Ernst, and Q. Hamid. 1997. Eosinophil-associated TGF-β1 mRNA expression and airways fibrosis in bronchial asthma. *Am. J. Respir. Cell Mol. Biol.* 17: 326–333.
8. Vignola, A. M., P. Chanez, G. Chiappara, A. Merendino, E. Pace, A. Rizzo, A. M. la Rocca, V. Bellia, G. Bonsignore, and J. Bousquet. 1997. Transforming growth factor-β expression in mucosal biopsies in asthma and chronic bronchitis. *Am. J. Respir. Crit. Care Med.* 156: 591–599.
9. Khalil, N., R. N. O'Connor, K. C. Flanders, and H. Unruh. 1996. TGF-β1, but not TGF-β2 or TGF-β3, is differentially present in epithelial cells of advanced pulmonary fibrosis: an immunohistochemical study. *Am. J. Respir. Cell Mol. Biol.* 14: 131–138.
10. Broekelmann, T. J., A. H. Limper, T. V. Colby, and J. A. McDonald. 1991. Transforming growth factor β1 is present at sites of extracellular matrix gene expression in human pulmonary fibrosis. *Proc. Natl. Acad. Sci. USA* 88: 6642–6646.
11. Kim, S. J., K. Park, D. Koeller, K. Y. Kim, L. M. Wakefield, M. B. Sporn, and A. B. Roberts. 1992. Post-transcriptional regulation of the human transforming growth factor-β1 gene. *J. Biol. Chem.* 267: 13702–13707.
12. Phillips, A. O., N. Topley, R. Steadman, K. Morrisey, and J. D. Williams. 1996. Induction of TGF-β1 synthesis in D-glucose primed human proximal tubular cells by IL-1β and TNFα. *Kidney Int.* 50: 1546–1554.
13. Phan, S. H., M. Gharaee-Kermani, B. McGarry, S. L. Kunkel, and F. W. Wolber. 1992. Regulation of rat pulmonary artery endothelial cell transforming growth factor-β production by IL-1β and tumor necrosis factor-α. *J. Immunol.* 149: 103–106.
14. Offner, F. A., H. Feichtinger, S. Stadlmann, P. Obrist, C. Marth, P. Klingler, B. Grage, M. Schmahl, and C. Knabbe. 1996. Transforming growth factor-β synthesis by human peritoneal mesothelial cells: induction by interleukin-1. *Am. J. Pathol.* 148: 1679–1688.
15. Kim, S. J., A. Glick, M. B. Sporn, and A. B. Roberts. 1989. Characterization of the promoter region of the human transforming growth factor-β1 gene. *J. Biol. Chem.* 264: 402–408.
16. Kim, S. J., P. Angel, R. Lafyatis, K. Hattori, K. Y. Kim, M. B. Sporn, M. Karin, and A. B. Roberts. 1990. Autoinduction of transforming growth factor β1 is mediated by the AP-1 complex. *Mol. Cell. Biol.* 10: 1492–1497.
17. Geiser, A. G., K. J. Busam, S. J. Kim, R. Lafyatis, M. A. O'Reilly, R. Webbink, A. B. Roberts, and M. B. Sporn. 1993. Regulation of the transforming growth factor-β1 and -β3 promoters by transcription factor Sp1. *Gene* 129: 223–228.
18. Rameshwar, P., R. Narayanan, J. Qian, T. N. Denny, C. Colon, and P. Gascon. 2000. NF-κB as a central mediator in the induction of TGF-β in monocytes from patients with idiopathic myelofibrosis: an inflammatory response beyond the realm of homeostasis. *J. Immunol.* 165: 2271–2277.
19. Perez, J. R., K. A. Higgins-Sochaski, J. Y. Maltese, and R. Narayanan. 1994. Regulation of adhesion and growth of fibrosarcoma cells by NF-κB RelA involves transforming growth factor β. *Mol. Cell. Biol.* 14: 5326–5332.
20. Strahl, B. D., and C. D. Allis. 2000. The language of covalent histone modifications. *Nature* 403: 41–45.
21. Ura, K., H. Kurumizaka, S. Dimitrov, G. Almouzni, and A. P. Wolffe. 1997. Histone acetylation: influence on transcription, nucleosome mobility and positioning, and linker histone-dependent transcriptional repression. *EMBO J.* 16: 2096–2107.
22. Wolffe, A. P. 1997. Transcriptional control: sinful repression. *Nature* 387: 16–17.
23. Ogryzko, V. V., R. L. Schiltz, V. Russanova, B. H. Howard, and Y. Nakatani. 1996. The transcriptional coactivators p300 and CBP are histone acetyltransferases. *Cell* 87: 953–959.
24. Yang, X. J., V. V. Ogryzko, J. Nishikawa, B. H. Howard, and Y. Nakatani. 1996. A p300/CBP-associated factor that competes with the adenoviral oncoprotein E1A. *Nature* 382: 319–324.
25. Agalioti, T., S. Lomvardas, B. Parekh, J. Yie, T. Maniatis, and D. Thanos. 2000. Ordered recruitment of chromatin modifying and general transcription factors to the IFN-β promoter. *Cell* 103: 667–678.
26. Wang, J. C., M. K. Derynck, D. F. Nonaka, D. B. Khodabakhsh, C. Haqq, and K. R. Yamamoto. 2004. Chromatin immunoprecipitation (ChIP) scanning identifies primary glucocorticoid receptor target genes. *Proc. Natl. Acad. Sci. USA* 101: 15603–15608.

27. Boukaba, A., E. I. Georgieva, F. A. Myers, A. W. Thorne, G. Lopez-Rodas, C. Crane-Robinson, and L. Franco. 2004. A short-range gradient of histone H3 acetylation and Tup1p redistribution at the promoter of the *Saccharomyces cerevisiae* SUC2 gene. *J. Biol. Chem.* 279: 7678–7684.
28. Muraoka, R. S., P. B. Bushdid, D. M. Brantley, F. E. Yull, and L. D. Kerr. 2000. Mesenchymal expression of nuclear factor-κB inhibits epithelial growth and branching in the embryonic chick lung. *Dev. Biol.* 225: 322–338.
29. Weigert, C., U. Sauer, K. Brodbeck, A. Pfeiffer, H. U. Haring, and E. D. Schleicher. 2000. AP-1 proteins mediate hyperglycemia-induced activation of the human TGF-β1 promoter in mesangial cells. *J. Am. Soc. Nephrol.* 11: 2007–2016.
30. Guo, Z., G. H. Boekhoudt, and J. M. Boss. 2003. Role of the intronic enhancer in tumor necrosis factor-mediated induction of manganous superoxide dismutase. *J. Biol. Chem.* 278: 23570–23578.
31. Saccani, S., S. Pantano, and G. Natoli. 2001. Two waves of nuclear factor κB recruitment to target promoters. *J. Exp. Med.* 193: 1351–1135.
32. Orphanides, G., and D. Reinberg. 2000. RNA polymerase II elongation through chromatin. *Nature* 407: 471–475.
33. Cho, H., G. Orphanides, X. Sun, X. J. Yang, V. Ogryzko, E. Lees, Y. Nakatani, and D. Reinberg. 1998. A human RNA polymerase II complex containing factors that modify chromatin structure. *Mol. Cell. Biol.* 18: 5355–5363.
34. Li, J., M. Gorospe, D. Hutter, J. Barnes, S. M. Keyse, and Y. Liu. 2001. Transcriptional induction of MKP-1 in response to stress is associated with histone H3 phosphorylation-acetylation. *Mol. Cell. Biol.* 21: 8213–8224.
35. Ng, K. W., P. Ridgway, D. R. Cohen, and D. J. Tremethick. 1997. The binding of a Fos/Jun heterodimer can completely disrupt the structure of a nucleosome. *EMBO J.* 16: 2072–2085.
36. Yue, T. L., X. K. Wang, B. Olson, and G. Feuerstein. 1994. Interleukin-1β (IL-1β) induces transforming growth factor-β (TGF-β1) production by rat aortic smooth muscle cells. *Biochem. Biophys. Res. Commun.* 204: 1186–1192.
37. Theodorescu, D., D. Bergsma, M. S. Man, N. Elshourbagy, C. Sheehan, D. Rieman, and R. S. Kerbel. 1991. Cloning and overexpression of TGF-β1 cDNA in a mammary adenocarcinoma: in vitro and in vivo effects. *Growth Factors* 5: 305–316.
38. Munger, J. S., J. G. Harpel, P. E. Gleizes, R. Mazzieri, I. Nunes, and D. B. Rifkin. 1997. Latent transforming growth factor-β: structural features and mechanisms of activation. *Kidney Int.* 51: 1376–1382.
39. Grainger, D. J., P. R. Kemp, A. C. Liu, R. M. Lawn, and J. C. Metcalfe. 1994. Activation of transforming growth factor-β is inhibited in transgenic apolipoprotein(a) mice. *Nature* 370: 460–462.
40. Crawford, S. E., V. Stellmach, J. E. Murphy-Ullrich, S. M. Ribeiro, J. Lawler, R. O. Hynes, G. P. Boivin, and N. Bouck. 1998. Thrombospondin-1 is a major activator of TGF-β1 in vivo. *Cell* 93: 1159–1170.
41. Munger, J. S., X. Huang, H. Kawakatsu, M. J. Griffiths, S. L. Dalton, J. Wu, J. F. Pittet, N. Kaminski, C. Garat, M. A. Matthay, et al. 1999. The integrin $\alpha_v\beta_6$ binds and activates latent TGFβ1: a mechanism for regulating pulmonary inflammation and fibrosis. *Cell* 96: 319–328.